Transition Path Sampling with Boltzmann Generator-based MCMC Moves

Michael Plainer[1]* **Hannes Stärk**[2]* **Charlotte Bunne**[3] **Stephan Günnemann**[1]

[1]School of Computation, Information and Technology, TUM
[2]Computer Science and Artificial Intelligence Laboratory, MIT
[3]Department of Computer Science, ETH Zürich

Abstract

Sampling all possible transition paths between two 3D states of a molecular system has various applications ranging from catalyst design to drug discovery. Current approaches to sample transition paths use Markov chain Monte Carlo and rely on time-intensive molecular dynamics simulations to find new paths. Our approach operates in the latent space of a normalizing flow that maps from the molecule's Boltzmann distribution to a Gaussian, where we propose new paths without requiring molecular simulations. Using alanine dipeptide, we explore Metropolis-Hastings acceptance criteria in the latent space for exact sampling and investigate different latent proposal mechanisms.

1 Introduction

Sampling the trajectories in which a molecular system changes from one 3D configuration to another—a task known as transition path sampling (TPS)—has many applications, such as designing catalysts [Crehuet and Field, 2007], materials [Selli et al., 2016], or drug discovery [Kirmizialtin et al., 2012, 2015]. In the TPS problem, we are given a single molecular system and two 3D conformations of interest for it: states A and B. These could be the structure of reactants before and the structure of the product molecule after the reaction. With this, we aim to sample transitions between and describe them with the likelihood at which they occur. To describe a transition path, withe use a sequence of time-equidistant 3D atom configurations (i.e., frames). that starts in state A and ends in state B.

Existing approaches for this problem [Dellago et al., 1998b,a, Bolhuis et al., 2002] use Markov chain Monte Carlo (MCMC) sampling to iteratively sample a new path given the current one. New paths are commonly proposed using shooting moves that require molecular dynamics simulation. Given a path, the proposal is generated by randomly selecting a frame, and sampling a random velocity from a Gaussian, and simulating the molecular dynamics. The selected frame with the new velocity is then simulated. If the simulation reaches state A and ends in state B, this trajectory constitutes a new non-zero probability transition path, which is accepted or rejected based on its probability and a Metropolis-Hastings [Metropolis et al., 1953, Hastings, 1970] acceptance criterion.

In this work, we explore how the TPS problem can be addressed when having access to a Boltzmann generator [Noé et al., 2019], which solves the easier problem of sampling the molecular systems distribution of 3D conformers. Given this, we generate MCMC proposals by first moving every frame in a path into our latent space. We modify each frame of this path and use the Boltzmann generator to bring the whole path back to configuration space and apply Metropolis-Hastings, as seen in Figure 1.

Our contributions are investigating this novel method for transition path sampling and highlighting its challenges. To that end, we describe the difficulty of calculating likelihoods for paths that were not generated with molecular dynamics and the obstacles for calculating path probabilities in parallel. Additionally, we provide insights into what configuration space paths are produced from simple paths in the latent space of a Boltzmann generator.

---

*Equal contribution. Correspondence to `michael.plainer@tum.de` and `hstark@mit.edu`.
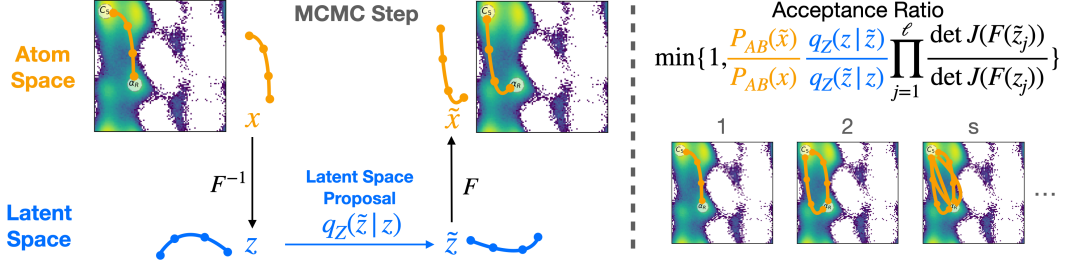
Figure 1: **MCMC proposals for latent space transition paths.** We move a transition path $\boldsymbol{x}$ into latent space using a Boltzmann generator $F(\cdot)$. With this path $\boldsymbol{z}$ and our latent space proposal kernel $q_Z(\tilde{\boldsymbol{z}} \mid \boldsymbol{z})$ we propose $\tilde{\boldsymbol{z}}$ and bring it back to configuration/atom space to obtain the transition path proposal $\tilde{\boldsymbol{x}}$. The likelihood of all steps can be computed, and we use them in a Metropolis-Hastings acceptance criterion to sample the transition path ensemble with MCMC.

2 Method

We assume access to a Boltzmann generator for the molecule of interest and two of its states, A and B, between which we wish to sample the transition path ensemble. In the following, we lay out the overall MCMC framework over latent space paths (see § 2.1). This requires two components: Calculating the path probability (see § 2.2), and a proposal kernel for a path in latent space for which we lay out several options (see § 2.3).

2.1 MCMC Framework for Latent Paths

Let $\boldsymbol{x}$ be our current path with frames $\boldsymbol{x}_i \in \mathbb{R}^{n \times 3}$ and $i \in \{1, ..., l\}$, where n is the number of atoms of our molecule and l the number of frames which we keep constant (the spacing of the frames can change with changing path lengths). For our MCMC procedure, we further need a proposal kernel $q(\tilde{\boldsymbol{x}} \mid \boldsymbol{x})$ that produces a new path proposal $\tilde{\boldsymbol{x}}$ from our current path $\boldsymbol{x}$. If we can additionally compute the probability of a path p_{AB}, we can sample the transition path ensemble with the MCMC algorithm using Metropolis-Hastings acceptance criterion

$$\alpha = \min \left\{ 1, \frac{p_{AB}\left(\tilde{\boldsymbol{x}}\right)}{p_{AB}(\boldsymbol{x})} \cdot \frac{q\left(\boldsymbol{x} \mid \tilde{\boldsymbol{x}}\right)}{q\left(\tilde{\boldsymbol{x}} \mid \boldsymbol{x}\right)} \right\}. \tag{1}$$

In our work, the proposal consists of first using a Boltzmann generator F trained on the molecule to move the path $\boldsymbol{x}$ into latent space to obtain the latent path $\boldsymbol{z} = \left\{ F^{-1}\left(\boldsymbol{x}_1\right), \ldots, F^{-1}\left(\boldsymbol{x}_l\right) \right\}$. Subsequently, we make a proposal in latent space to obtain a new latent path $\tilde{\boldsymbol{z}}$ using the latent proposal kernel $q_Z(\tilde{\boldsymbol{z}} \mid \boldsymbol{z})$ which we design in § 2.3. Lastly, the latent path is projected back to configuration space using the Boltzmann generator $\boldsymbol{x} = \{F\left(\tilde{\boldsymbol{z}}_1\right), \ldots, F\left(\tilde{\boldsymbol{z}}_l\right)\}$.

The ratio of the path proposal probabilities in configuration space can be equivalently written by the latent space proposal probability (compare Appendix B.1) as

$$\frac{q(\boldsymbol{x} \mid \tilde{\boldsymbol{x}})}{q(\tilde{\boldsymbol{x}} \mid \boldsymbol{x})} = \frac{q_Z(\boldsymbol{z} \mid \tilde{\boldsymbol{z}})}{q_Z(\tilde{\boldsymbol{z}} \mid \boldsymbol{z})} \cdot \prod_{i=1}^{l} \frac{|\det J(F\left(\tilde{\boldsymbol{z}}_i\right))|}{|\det J(F\left(\boldsymbol{z}_i\right))|}, \tag{2}$$

where the Jacobian J accounts for the change of density when moving the path to latent space. We can use this ratio readily to calculate the acceptance ratio for the MCMC algorithm as laid out in Algorithm 1. The remaining challenges are the ability to compute the path probability p_{AB} and a concrete latent space proposal kernel $q_Z(\tilde{\boldsymbol{z}} \mid \boldsymbol{z})$, which we will tackle next.

2.2 Calculating the Path Probability

A path's probability is defined with respect to a molecular dynamics model. Here, we assume Langevin where we omit the constant atom masses and friction coefficient for the sake of brevity. The transition from frame $\boldsymbol{x}_i$ to the next frame $\boldsymbol{x}_{i+1}$ can be calculated as

$$\boldsymbol{x}_{i+1} = \boldsymbol{x}_i + \Delta t \boldsymbol{v}_{i+1}$$
$$\boldsymbol{v}_{i+1} = \alpha \boldsymbol{v}_i + (1-\alpha)\nabla U(\boldsymbol{x}_i) + \sqrt{k_B T(1-\alpha^2)}\boldsymbol{W}, \tag{3}$$

given the velocity $\boldsymbol{v}_i$, and the molecule's energy function $U : \mathbb{R}^{d \times 3} \mapsto \mathbb{R}$. $\alpha = \exp(-\Delta t)$ for a time step size Δt and $\boldsymbol{W} \sim \mathcal{N}(0, \mathbb{1})$ corresponds to random motion that is scaled proportional to the Boltzmann constant k_B and temperature T. Notice that in Langevin dynamics, the only randomness when obtaining $\boldsymbol{x}_{i+1}$ from $\boldsymbol{x}_i$ given the velocity $\boldsymbol{v}_i$ stems from the Gaussian variable $\sqrt{k_B T (1 - \alpha^2)} \boldsymbol{W}$. Thus, the probability density $p(\boldsymbol{x}_{i+1}, \boldsymbol{v}_{i+1} \mid \boldsymbol{x}_i, \boldsymbol{v}_i)$ of moving from $\boldsymbol{x}_i$ to $\boldsymbol{x}_{i+1}$ is that of a Gaussian with mean $\mu = \boldsymbol{x}_i + \Delta t (\alpha \boldsymbol{v}_i + (1 - \alpha) \nabla U(\boldsymbol{x}_i))$ and a standard deviation of $\sigma = \Delta t^2 k_B T (1 - \alpha^2)$.

Given this probability $p(\boldsymbol{x}_{i+1}, \boldsymbol{v}_{i+1} \mid \boldsymbol{x}_i, \boldsymbol{v}_i)$ of moving between individual frames with the auxiliary velocity variable, the probability of a whole path in configuration space is

$$p_{AB}(\boldsymbol{x}) = p(\boldsymbol{x}_1) \cdot \rho(\boldsymbol{v}_1) \cdot \prod_{i=1}^{l-1} p(\boldsymbol{x}_{i+1}, \boldsymbol{v}_{i+1} \mid \boldsymbol{x}_i, \boldsymbol{v}_i), \tag{4}$$

where $p(\boldsymbol{x}_1)$ follows the molecule's Boltzmann distribution, meaning that $p(\boldsymbol{x}_i) \propto \exp(-U(\boldsymbol{x}_i)/k_B T)$ with an unknown proportionality constant. However, this constant is unnecessary since it will cancel out with the same constant of the reverse path density p_{BA} in the acceptance ratio in Equation 1. $\rho(\boldsymbol{v}_1)$ is the probability of $\boldsymbol{v}_1$ and is typically $\mathcal{N}(\mathbf{0}, \operatorname{diag}(k_B T))$ [Castellan, 1983].

Thus, the last missing link to computing $p_{AB}(\boldsymbol{x})$ is the initial velocity $\boldsymbol{v}_1$. Since our path definition does not include an initial velocity (because we do not have a Boltzmann generator that operates over both velocities and positions), we opt to marginalize over all possible velocities and approximate the following expectation as our final path probability

$$p_{AB}(\boldsymbol{x}) = \mathbb{E}_{\boldsymbol{v}_1 \sim \mathcal{N}(\mathbf{0}, \operatorname{diag}(k_B T))} \left[p(\boldsymbol{x}_1) \cdot \prod_{i=1}^{l-1} p(\boldsymbol{x}_{i+1}, \boldsymbol{v}_{i+1} \mid \boldsymbol{x}_i, \boldsymbol{v}_i) \right]. \tag{5}$$

All subsequent velocities $\{\boldsymbol{v}_i\}_{i \in \{2, \ldots, l\}}$ can then be inferred by solving the previous step, allowing us to compute $p(\boldsymbol{x}_{i+1}, \boldsymbol{v}_{i+1} \mid \boldsymbol{x}_i, \boldsymbol{v}_i)$ sequentially.

Desirable properties. In designing our MCMC procedure, we set out to avoid the time-consuming sequential molecular dynamics simulation. While the path probability can be computed easily for paths generated by MD [Jung et al., 2017], calculating the path probability $p_{AB}(\boldsymbol{x})$ still requires some sequential computation in our approach. However, this amounts to sequentially performing l vector additions, which is very cheap and can be done in parallel for all different initial velocities when approximating the expectation. The expensive, time-consuming computations stem from the evaluation of the energy function $U(\boldsymbol{x}_i)$ for each frame. In our procedure, this can be done in parallel, while in molecular dynamics, it has to be performed sequentially.

2.3 Latent Space Path Proposal Kernel

As for the concrete latent space path proposal kernel $q_Z(\tilde{\boldsymbol{z}} \mid \boldsymbol{z})$, we propose three different options: 1) Gaussian noise added to each frame. 2) A Gaussian Process (GP) with the current path as its mean. 3) A GP that is adaptively fit to the history of all sampled transition paths and only weakly depends on the current path. All these proposals are symmetric and will not contribute to our acceptance ratio with $q_Z(\tilde{\boldsymbol{z}} \mid \boldsymbol{z}) \, / \, q_Z(\boldsymbol{z} \mid \tilde{\boldsymbol{z}}) = 1$.

Gaussian proposal. From a latent path $\boldsymbol{z}$, we propose a new path $\tilde{\boldsymbol{z}} = \{\boldsymbol{z}_1 + \epsilon_1, \ldots, \boldsymbol{z}_l + \epsilon_l\}$ where $\epsilon_1, \ldots, \epsilon_l \sim \mathcal{N}(\mathbf{0}, \boldsymbol{\Sigma})$. While this independent noise for each frame makes it unlikely that all frames move coherently and produce high-probability paths, this operation can be performed efficiently and allows for fast exploration of the latent space.

Conditional Gaussian process path proposals. We employ a GP $f(t) \sim \mathcal{GP}(m(t), k(t, t'))$, where $f : \mathbb{R} \mapsto \mathbb{R}^{3n-6}$ maps the time $t \in [1, l]$ along the path to a Gaussian from which a frame at time t is sampled[2]. We fit the GP mean $m(\cdot)$ and kernel function $k(\cdot, \cdot)$, which is not to be confused with the proposal kernel, to a set of s latent paths $\{\boldsymbol{z}^i\}_{i \in \{1, \ldots s\}}$, where the index of each frame is used as the time t. Our set of latent paths $\{\boldsymbol{z}^i\}_{i \in \{1, \ldots s\}}$ to fit the GP is the history of all accepted paths.

When using the history $\{\boldsymbol{z}^i\}_{i \in \{1, \ldots s\}}$, the proposal kernel $\mathcal{GP}_s$ changes over the course of MCMC steps s, leading to an adaptive MCMC algorithm. For this to be correct, the proposal kernel has to

---

[2]The latent space dimensionality is $\mathbb{R}^{3n-6}$ for n atoms since the Boltzmann generator operates on internal coordinates that are invariant to the 6 degrees of freedom from rigid translations and rotations.
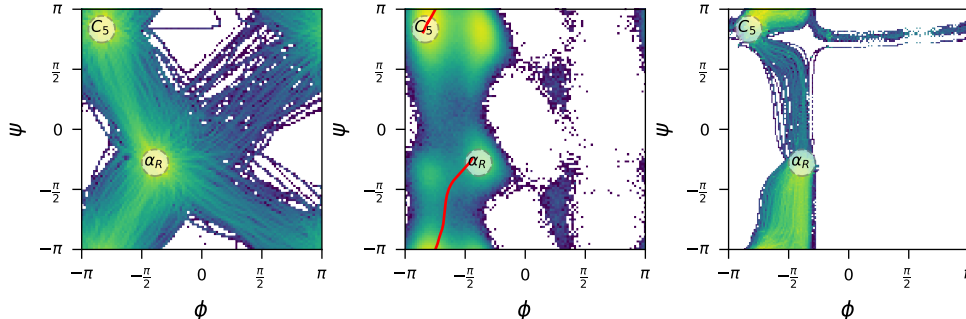
Figure 2: **Linear (latent space) interpolation.** *Left*: A histogram of the two main dihedral angels ϕ, ψ when linearly interpolating the atom coordinates of configurations from the state C_5 and α_R in product space. *Center*: A histogram of the states occurring in the MD simulation and a linear interpolation in latent space (red line) are shown. *Right*: The resulting density of transition paths when linearly interpolating between those states in latent space.

converge and satisfy vanishing adaptation [Andrieu and Thoms, 2008] where, as the Markov chain progresses, the influence of its most recent states on the proposal kernel has to diminish. Intuitively, this is the case for our adaptive kernel since the influence of the most recent path on the fitted mean and covariance kernel vanishes as the size of the history (the Markov chain) increases.

We re-fit this adaptive GP proposal to the history of latent paths $\{z^i\}_{i \in \{1,...s\}}$ at each step s when a new path has been accepted. To efficiently do so, we start optimization from the parameters of the previous GP proposal kernel that are optimal for $\{z^i\}_{i \in \{1,...s-1\}}$. The new optimization's convergence is typically fast since the minimum under the new set of latent paths at step s is likely close to that at step $s - 1$, with the difference diminishing as the length of the Markov chain increases.

Given the fitted GP, a new latent path $\tilde{z}$ is proposed conditioned on the current one z by sampling $\mathcal{GP}_s$ at times $t = 1, \ldots, l$ (i.e., the frame numbers) after setting the means of $\mathcal{GP}_s$ at those times to the frames of z, meaning that $m(t) = z_t$ for $t \in \{1, \ldots l\}$. This amounts to sampling $\mathcal{GP}_s$ unconditionally at $t = 1, \ldots, l$, subtracting the means $m(t)$, and adding the frames z_t at each time.

Unconditional Gaussian process path proposals. Here, we use the adaptive Gaussian process $\mathcal{GP}_s$ and propose new paths $\tilde{z}$ unconditionally, meaning that each proposal is a sample of $\mathcal{GP}_s$ and the only influence of z is through its presence in the set of paths $\{z^i\}_{i \in \{1,...s\}}$ that $\mathcal{GP}_s$ was fit on. This means that with a progressively increasing number of accepted paths, the influence of the current path will diminish, thus satisfying the requirements for an adaptive MCMC kernel. We note that in the limit of samples, the Gaussian process itself can be used to sample transition paths without MCMC.

Further, we can also evaluate $\mathcal{GP}_s$ at times between the integer times of the frames. This allows us to introduce more variance by evaluating the Gaussian process not at the fixed points $1, \ldots, l$, but to uniformly draw l sorted samples from $\mathcal{U}_{[0.5,l+0.5]}$, to can change the spacing of individual frames.

3 Experiments

Ground truth ensemble. We use two ground truth definitions to compare with. In the first, we simulate 10 nanoseconds of ALDP dynamics with a timestep of 1 femtosecond at 300K with the openMM MD engine [Eastman et al., 2017]. The ground truth TP ensemble is then defined as all sequences of that MD trajectory that start in A and transition to B (or vice versa). Only the shortest transitions are included, so if a trajectory reenters a state, it is discarded. This approach extracts variable-length transition paths from a long-running MD simulation.

For the second ground truth ensemble, we use a fixed path length ensemble. We obtain it using the two-way shooting move MCMC algorithm implemented in the open path sampling library [Swenson et al., 2018a,b] with the same molecular dynamics setup as above. The ground truth ensembles show how rare transitions (Figure 3 bottom) are particularly difficult to produce with classical MD, already for the small molecule alanine dipeptide.

Latent space analysis. When moving configurations from the meta-stable states C_5 and α_R of alanine dipeptide (ALDP) into the latent space, we can linearly interpolate between them and map them back with the trained Boltzmann generator. Figure 2 shows that linear paths in latent space

produce non-linear paths in configuration space. Surprisingly, this naive latent space interpolation already gives rise to two separate transition channels in configuration space.

Results. Figure 3 shows for all methods a histogram of the sampled transition paths between the states $C_5 \leftrightarrow \alpha_R$ and $\alpha_R \leftrightarrow C_7$, respectively. *Unconditional GP Uni* refers to the adaptive GP proposal with uniform timepoint sampling while *Unconditional GP* always samples the index of the frame as timepoint. *Conditional GP* uses the adaptive proposal.

The main finding is that due to the low acceptance rate of our MCMC steps, we are only able to produce a low amount of paths or a set of paths with low diversity. When increasing the variance, paths are more diverse but also less likely to be accepted. To overcome this, proposals that produce more likely paths while maintaining diversity are required. Our various latent space proposal kernels seem insufficient.

While training a fixed Gaussian process on simple paths in latent space is computationally favorable, the results do not indicate that it can capture the transition paths. In general, we have seen in our experiments that the selection for a kernel of the Gaussian process (compare Appendix B.3) poses a difficult problem for this task because it must capture an adequate amount of noise without overfitting to the previous paths.

Overall, the results qualitatively show that the simplest proposal kernel, one that simply adds Gaussian noise in latent space, appears to be the most efficient and effective choice. Further, conditioning the Gaussian process on the current path appears to slightly increase the variance and leads to a more diverse set of paths.

The code for our experiments is available at `https://github.com/plainerman/Latent-TPS`.
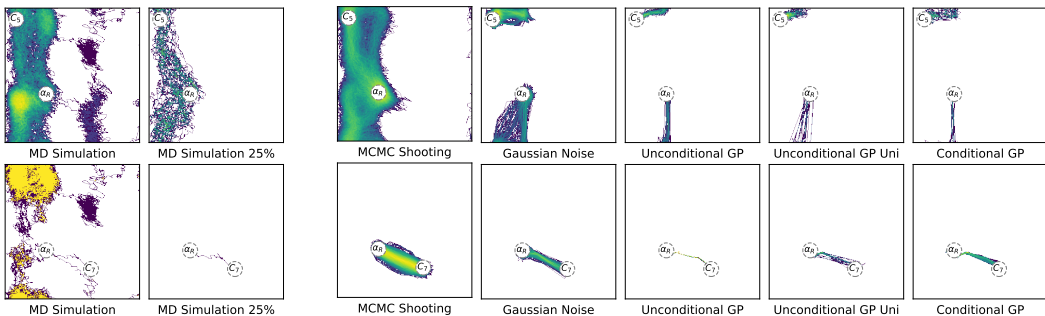

Figure 3: **Comparison of sampling methods**. Each row shows the transitions between two different metastable states. *Left:* "Ground truth" path ensemble from MD simulation of all paths (sub-left) and the 25% of paths with the highest probability (sub-right). *Right:* Shooting move MCMC ensemble and the ensembles of our different latent space proposal kernels. Note that it is unclear what a meaningful ground truth ensemble is.

4   Discussion and Conclusion

Limitations. Our approach relies on a trained Boltzmann generator, of which high-quality ones for larger molecular systems do not exist yet. Furthermore, the latent space path proposal kernels we devise have too low acceptance rates to be useful. This limits them to a low variance, slowing down mode-mixing. Better latent space proposals would be necessary. Lastly, an avenue toward a practical solution could be adaptively fine-tuning the Boltzmann generator to make simple paths in latent space correspond to physical paths that obey Langevin dynamics in configuration space.

Conclusion. In this paper, we presented a novel way to propose transition paths in the latent space of a Boltzmann generator. Throughout this work, we have introduced multiple latent space path proposal kernels that perform (learned) operations. This enables a transition path sampling MCMC procedure without the need for molecular dynamics simulation. We believe that learned transition path sampling methods and, in general, simulation-free MCMC approaches are interesting research questions to explore and might lead to faster sampling methods.

Acknowledgments and Disclosure of Funding

References

Christophe Andrieu and Johannes Thoms. A tutorial on adaptive mcmc. *Statistics and Computing*, 18(4):343–373, Dec 2008.

Peter G. Bolhuis, David Chandler, Christoph Dellago, and Phillip L. Geissler. Transition path sampling: Throwing ropes over rough mountain passes, in the dark. *Annual Review of Physical Chemistry*, 53(1):291–318, October 2002.

Gilbert William Castellan. *Physical Chemistry*. Addison-Wesley, Reading, Mass, 3rd ed edition, 1983.

Ramon Crehuet and Martin J. Field. A transition path sampling study of the reaction catalyzed by the enzyme chorismate mutase. *The Journal of Physical Chemistry B*, 111(20):5708–5718, May 2007.

Christoph Dellago, Peter G. Bolhuis, and David Chandler. Efficient transition path sampling: Application to lennard-jones cluster rearrangements. *The Journal of Chemical Physics*, 108(22): 9236–9245, June 1998a.

Christoph Dellago, Peter G. Bolhuis, Félix S. Csajka, and David Chandler. Transition path sampling and the calculation of rate constants. *The Journal of Chemical Physics*, 108(5):1964–1977, 02 1998b.

Laurent Dinh, Jascha Sohl-Dickstein, and Samy Bengio. Density estimation using real NVP. In *International Conference on Learning Representations*, 2017.

Simon Duane, A.D. Kennedy, Brian J. Pendleton, and Duncan Roweth. Hybrid monte carlo. *Physics Letters B*, 195(2):216–222, 1987.

Conor Durkan, Artur Bekasov, Iain Murray, and George Papamakarios. Neural spline flows. In H. Wallach, H. Larochelle, A. Beygelzimer, F. d'Alché-Buc, E. Fox, and R. Garnett, editors, *Advances in Neural Information Processing Systems*, volume 32. Curran Associates, Inc., 2019.

Peter Eastman, Jason Swails, John D. Chodera, Robert T. McGibbon, Yutong Zhao, Kyle A. Beauchamp, Lee-Ping Wang, Andrew C. Simmonett, Matthew P. Harrigan, Chaya D. Stern, Rafal P. Wiewiora, Bernard R. Brooks, and Vijay S. Pande. OpenMM 7: Rapid development of high performance algorithms for molecular dynamics. *PLOS Computational Biology*, 13(7): e1005659, July 2017.

Sebastian Falkner, Alessandro Coretti, Salvatore Romano, Phillip Geissler, and Christoph Dellago. Conditioning normalizing flows for rare event sampling, 2023.

W. K. Hastings. Monte carlo sampling methods using markov chains and their applications. *Biometrika*, 57(1):97–109, April 1970.

Matthew Hoffman, Pavel Sountsov, Joshua V. Dillon, Ian Langmore, Dustin Tran, and Srinivas Vasudevan. Neutra-lizing bad geometry in hamiltonian monte carlo using neural transport, 2019.

Lars Holdijk, Yuanqi Du, Ferry Hooft, Priyank Jaini, Bernd Ensing, and Max Welling. Stochastic optimal control for collective variable free sampling of molecular transition paths, 2023.

Hendrik Jung, Kei ichi Okazaki, and Gerhard Hummer. Transition path sampling of rare events by shooting from the top. *The Journal of Chemical Physics*, 147(15), August 2017.

Hendrik Jung, Roberto Covino, A. Arjun, Christian Leitold, Christoph Dellago, Peter G. Bolhuis, and Gerhard Hummer. Machine-guided path sampling to discover mechanisms of molecular self-organization. *Nature Computational Science*, 3(4):334–345, April 2023.

Serdal Kirmizialtin, Virginia Nguyen, Kenneth A. Johnson, and Ron Elber. How conformational dynamics of DNA polymerase select correct substrates: Experiments and simulations. *Structure*, 20(4):618–627, April 2012.

Serdal Kirmizialtin, Kenneth A. Johnson, and Ron Elber. Enzyme selectivity of HIV reverse transcriptase: Conformations, ligands, and free energy partition. *The Journal of Physical Chemistry B*, 119(35):11513–11526, August 2015.

Tianyi Liu, Weihao Gao, Zhirui Wang, and Chong Wang. Pathflow: A normalizing flow generator that finds transition paths. In James Cussens and Kun Zhang, editors, *Proceedings of the Thirty-Eighth Conference on Uncertainty in Artificial Intelligence*, volume 180 of *Proceedings of Machine Learning Research*, pages 1232–1242. PMLR, 01–05 Aug 2022.

Nicholas Metropolis, Arianna W. Rosenbluth, Marshall N. Rosenbluth, Augusta H. Teller, and Edward Teller. Equation of state calculations by fast computing machines. *The Journal of Chemical Physics*, 21(6):1087–1092, June 1953.

Laurence I. Midgley, Vincent Stimper, Javier Antorán, Emile Mathieu, Bernhard Schölkopf, and José Miguel Hernández-Lobato. Se(3) equivariant augmented coupling flows, 2023a.

Laurence Illing Midgley, Vincent Stimper, Gregor N. C. Simm, Bernhard Schölkopf, and José Miguel Hernández-Lobato. Flow annealed importance sampling bootstrap. In *International Conference on Learning Representations*, 2023b.

Radford M. Neal. Mcmc using hamiltonian dynamics. In Steve Brooks, Andrew Gelman, Galin Jones, and Xiao-Li Meng, editors, *Handbook of Markov Chain Monte Carlo*. Chapman and Hall/CRC, 2011.

Frank Noé, Simon Olsson, Jonas Köhler, and Hao Wu. Boltzmann generators: Sampling equilibrium states of many-body systems with deep learning. *Science*, 365(6457), September 2019.

Danilo Jimenez Rezende, George Papamakarios, Sebastien Racaniere, Michael Albergo, Gurtej Kanwar, Phiala Shanahan, and Kyle Cranmer. Normalizing flows on tori and spheres. In *International Conference on Machine Learning*, pages 8083–8092. PMLR, 2020.

Daniele Selli, Salah Eddine Boulfelfel, Philipp Schapotschnikow, Davide Donadio, and Stefano Leoni. Hierarchical thermoelectrics: crystal grain boundaries as scalable phonon scatterers. *Nanoscale*, 8 (6):3729–3738, 2016.

David W. H. Swenson, Jan-Hendrik Prinz, Frank Noe, John D. Chodera, and Peter G. Bolhuis. OpenPathSampling: A python framework for path sampling simulations. 1. basics. *Journal of Chemical Theory and Computation*, 15(2):813–836, October 2018a.

David W. H. Swenson, Jan-Hendrik Prinz, Frank Noe, John D. Chodera, and Peter G. Bolhuis. OpenPathSampling: A python framework for path sampling simulations. 2. building and customizing path ensembles and sample schemes. *Journal of Chemical Theory and Computation*, 15(2): 837–856, October 2018b.

E. G. Tabak and Cristina V. Turner. A family of nonparametric density estimation algorithms. *Communications on Pure and Applied Mathematics*, 66(2):145–164, 2013.

Esteban G. Tabak and Eric Vanden-Eijnden. Density estimation by dual ascent of the log-likelihood. *Communications in Mathematical Sciences*, 8(1):217–233, 2010.

A Background and Related Work

Boltzmann generators. Given a molecule, the probability of each 3D configuration is proportional to the exponential of its negative energy, i.e., they follow a Boltzmann distribution. Noé et al. [2019] train a normalizing flow [Tabak and Vanden-Eijnden, 2010, Tabak and Turner, 2013] to sample a molecule's Boltzmann distribution, known as Boltzmann generator. While recent innovations [Midgley et al., 2023b,a] improved their training efficiency, training them for larger systems remains an open problem and a limitation of our Boltzmann generator-based approach.

Deep learning for transition path sampling. The TPS problem, with the goal to sample the whole transition path ensemble, is more challenging than finding a single low-energy transition path: A problem that also has been explored with deep learning (DL) approaches [Liu et al., 2022, Holdijk et al., 2023]. For the harder TPS problem, DL methods require MCMC with shooting moves as proposed by Dellago et al. [1998b,a]. For instance, Falkner et al. [2023] replace the shooting point selection with DL and sample them with a Boltzmann generator. Similarly, Jung et al. [2023] increase the acceptance rate of shooting moves by selecting the frames to shoot from with a learned function. These approaches still require sequential MD simulation. In this work, we explore a novel molecular dynamics-free MCMC paradigm using DL.

B Method Details

B.1 Latent Space Proposal Ratio

The proposal kernel takes the form $q(\tilde{\boldsymbol{x}} \mid \boldsymbol{x}) = p(\boldsymbol{z} \mid \boldsymbol{x})q_Z(\tilde{\boldsymbol{z}} \mid \boldsymbol{z})p(\tilde{\boldsymbol{x}} \mid \tilde{\boldsymbol{z}})$, where $p(\boldsymbol{z} \mid \boldsymbol{x})$ accounts for the change of density when using our Boltzmann generator to move the path $\boldsymbol{x}$ into latent space and $p(\tilde{\boldsymbol{x}} \mid \tilde{\boldsymbol{z}})$ arises from moving the new latent path back to configuration space. Since the Boltzmann generator processes all the frames independently, the change of density factors can be written as the product of the individual frames $p(\boldsymbol{z} \mid \boldsymbol{x}) = \prod_{i=1}^{l} p(\boldsymbol{z}_i \mid \boldsymbol{x}_i)$. With this in mind, the ratio of the forward path proposal $q(\tilde{\boldsymbol{x}} \mid \boldsymbol{x})$ and the backward proposal $q(\boldsymbol{x} \mid \tilde{\boldsymbol{x}})$, as it is required in the acceptance criterion in Equation 1, takes the form

$$\frac{q(\boldsymbol{x} \mid \tilde{\boldsymbol{x}})}{q(\tilde{\boldsymbol{x}} \mid \boldsymbol{x})} = \frac{q_Z(\boldsymbol{z} \mid \tilde{\boldsymbol{z}})}{q_Z(\tilde{\boldsymbol{z}} \mid \boldsymbol{z})} \cdot \prod_{i=1}^{l} \frac{p(\tilde{\boldsymbol{z}}_i \mid \tilde{\boldsymbol{x}}_i)p(\boldsymbol{x}_i \mid \boldsymbol{z}_i)}{p(\boldsymbol{z}_i \mid \boldsymbol{x}_i)p(\tilde{\boldsymbol{x}}_i \mid \tilde{\boldsymbol{z}}_i)}. \tag{6}$$

Each term in the product can be simplified as follows, where we write $\boldsymbol{x}, \boldsymbol{z}$ for an individual frame $\boldsymbol{x}_i, \boldsymbol{z}_i$ and use the change of variables formula $p(\boldsymbol{x}) = p(\boldsymbol{z}) \cdot |\det J(F(\boldsymbol{z}))|^{-1}$ in the third equality

$$\frac{p(\tilde{\boldsymbol{z}} \mid \tilde{\boldsymbol{x}})p(\boldsymbol{x} \mid \boldsymbol{z})}{p(\boldsymbol{z} \mid \boldsymbol{x})p(\tilde{\boldsymbol{x}} \mid \tilde{\boldsymbol{z}})} = \frac{\frac{p(\tilde{\boldsymbol{x}},\tilde{\boldsymbol{z}})}{p(\tilde{\boldsymbol{x}})}\frac{p(\boldsymbol{x},\boldsymbol{z})}{p(\boldsymbol{z})}}{\frac{p(\boldsymbol{x},\boldsymbol{z})}{p(\boldsymbol{x})}\frac{p(\tilde{\boldsymbol{x}},\tilde{\boldsymbol{z}})}{p(\tilde{\boldsymbol{z}})}} = \frac{p(\boldsymbol{x})p(\tilde{\boldsymbol{z}})}{p(\tilde{\boldsymbol{x}})p(\boldsymbol{z})} = \frac{p(\boldsymbol{z}) \left|\det J(F(\boldsymbol{z}))\right|^{-1} p(\tilde{\boldsymbol{z}})}{p(\tilde{\boldsymbol{z}}) \left|\det J(F(\tilde{\boldsymbol{z}}))\right|^{-1} p(\boldsymbol{z})} = \frac{\left|\det J(F(\tilde{\boldsymbol{z}}))\right|}{\left|\det J(F(\boldsymbol{z}))\right|}. \tag{7}$$

Thus, the ratio of proposals we need to calculate can be reformulated as

$$\frac{q(\boldsymbol{x} \mid \tilde{\boldsymbol{x}})}{q(\tilde{\boldsymbol{x}} \mid \boldsymbol{x})} = \frac{q_Z(\boldsymbol{z} \mid \tilde{\boldsymbol{z}})}{q_Z(\tilde{\boldsymbol{z}} \mid \boldsymbol{z})} \cdot \prod_{i=1}^{l} \frac{\left|\det J(F(\tilde{\boldsymbol{z}}_i))\right|}{\left|\det J(F(\boldsymbol{z}_i))\right|}. \tag{8}$$

B.2 Latent Path MCMC Algorithm

Our latent space path sampling approach builds on the Metropolis-Hastings method but relies on a modified acceptance criteria and an adapted proposal kernel.

B.3 Gaussian Process Kernel

A Gaussian process fits the parameters of a kernel k. As for the concrete choice of kernel, we have decided to use an RBF-Kernel with an additional white kernel that can capture variance in the individual points. It can be formulated as

$$k(x, x') = c \cdot \exp\left(-\frac{\|x - x'\|_2^2}{2l^2}\right) + n \cdot \mathbb{1}_{x \neq x'}, \tag{9}$$

with learnable parameters l, c, n.

Algorithm 1: Fixed-length latent space transition path sampling.

Input: Initial path $\boldsymbol{x}^{(0)}$ with l frames, a trained Boltzmann generator consisting of the map F and its inverse F^{-1}, the number of steps to run N, and a latent proposal kernel K with proposal probability $q_Z (\cdot \mid \cdot)$.

Output: MCMC samples following target distribution $\left\{ \boldsymbol{x}^{(1)}, \ldots, \boldsymbol{x}^{(N)} \right\}$.

1 Calculate latent space representation of initial path $\boldsymbol{z}^{(0)} = \left\{ F^{-1} \left(\boldsymbol{x}_1^{(0)} \right), \ldots, F^{-1} \left(\boldsymbol{x}_l^{(0)} \right) \right\}$.

2 **for** $i \leftarrow 1 \ldots N$ **do**

3   **repeat**

4   Propose new path in latent space $\tilde{z} = K \left(\boldsymbol{z}^{(i-1)} \right)$.

5   Compute the proposed path in configuration space $\tilde{\boldsymbol{x}} = \{ F (\tilde{z}_1), \ldots, F (\tilde{z}_l) \}$.

6   Compute acceptance probability

$$\alpha = \min \left\{ 1, \frac{p_{AB} (\tilde{\boldsymbol{x}})}{p_{AB} \left(\boldsymbol{x}^{(i-1)} \right)} \cdot \frac{q_Z \left(\boldsymbol{z}^{(i-1)} \mid \tilde{z} \right)}{q_Z \left(\tilde{z} \mid \boldsymbol{z}^{(i-1)} \right)} \cdot \prod_{j=1}^{l} \frac{|\det J (F (\tilde{z}_j))|}{\left| \det J \left(F(\boldsymbol{z}_j^{(i-1)}) \right) \right|} \right\} .$$

7   Draw a uniformly distributed random number $u \sim \mathcal{U}_{[0,1]}$.

8   **until** *proposed path $\tilde{\boldsymbol{x}}$ is reactive **and** $u \leq \alpha$*;

9   Accept proposed path $\boldsymbol{z}^{(i)} = \tilde{z}, \boldsymbol{x}^{(i)} = \tilde{\boldsymbol{x}}$.

10 **end**

B.4 Fixed Gaussian Process

Our set of latent paths $\{ \boldsymbol{z}^i \}_{i \in \{1, \ldots s\}}$ to fit the GP can either be the history of all previously sampled paths or we obtain it via linear interpolation in latent space. Specifically, to obtain an interpolation, we sample a start $\boldsymbol{x}_1$ and an end frame $\boldsymbol{x}_l$ from states A and B, move them to latent space to generate $\boldsymbol{z}_1, \boldsymbol{z}_l = F^{-1}(\boldsymbol{x}_1), F^{-1}(\boldsymbol{x}_l)$, and produce the latent path as the linear interpolation $\boldsymbol{z}_i = \frac{i}{l} \boldsymbol{z}_1 + (1 - \frac{i}{l}) \boldsymbol{z}_l$ for $i \in \{1, \ldots, l\}$. After moving it back to configuration space with the Boltzmann generator, this constitutes a coarse path. This produces a fixed proposal kernel, where the quality depends on the paths it was trained on. While training a fixed Gaussian process on simple paths in latent space is computationally favorable, it is a challanging task. First, the paths it is trained on need to be representative. Secondly, this fixed Gaussian process would allow us to sample transition path without conditioning on the current path.

B.5 Boltzmann Generator Training

We trained a Boltzmann generator F on the molecule ALDP, consisting of multiple neural spline layers [Durkan et al., 2019] with a randomly masked coupling architecture between them. The coupling layers allow us to use arbitrarily complex neural networks, that do not have to be invertible while still allowing the overall function to be invertible [Dinh et al., 2017]. In this architecture, the neural network learns to predict 8 knots and the parameters of a quadratic rational spline function. Overall, we use 12 of these neural spline coupling layers each using a residual block with two layers with 256 hidden units. The performance of the trained Boltzmann generator is illustrated in Figure 4.

To train the normalizing flow, we use the samples from the long-running MD simulation of ALDP and maximize the likelihood of the frames in latent space is. The goal of the loss is that the samples in latent space are distributed according to the base distribution. This is achieved by minimizing the forward KL divergence

$$\mathcal{L}_{KL} (\boldsymbol{\theta}) \propto -\mathbb{E}_{x \sim X} \left[\log \left(p_u \left(F_{\boldsymbol{\theta}}^{-1}(x) \right) \right) - \log \left| \det J \left(F_{\boldsymbol{\theta}}^{-1}(x) \right) \right| \right] . \tag{10}$$

J represents the Jacobian and p_u is the distribution of our latent space. F represents the invertible function of the Botlzmann generator that maps between the ground truth data distribution X and is parameterized by $\boldsymbol{\theta}$.

To represent the molecule, we rely on an internal coordinate representation for our flow, which describes the molecule's state by the dihedral angles and bond lengths [Rezende et al., 2020] as this
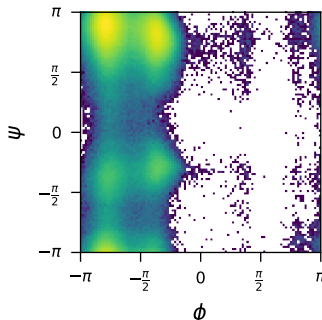
Figure 4: **Histogram of states sampled by Boltzmann generator.** This histogram shows the main dihedral angles of 1 million ALDP conformations sampled from the base distribution and then transported with the normalizing flow.

has shown good performance [Noé et al., 2019, Midgley et al., 2023b]. Since some of these variables are periodic, we use a mixture between a Gaussian and a uniform distribution as the base distribution. This mixture is only used for training; at inference, we change this to a standard normal distributed space by using the cumulative and inverse cumulative function to map uniform values from and to a normal distribution.

B.6   Further Latent Space Investigation

To ensure that the learned latent space is meaningful and can separate between different meta-stable states, we have reduced samples of the states C_5 and α_R to two dimensions, as seen in Figure 5. Already a PCA, a non-linear dimensionality reduction, is capable the separating the states by a single dimension. This motivates that a linear interpolation between configurations in latent space can produce feasible transition paths.
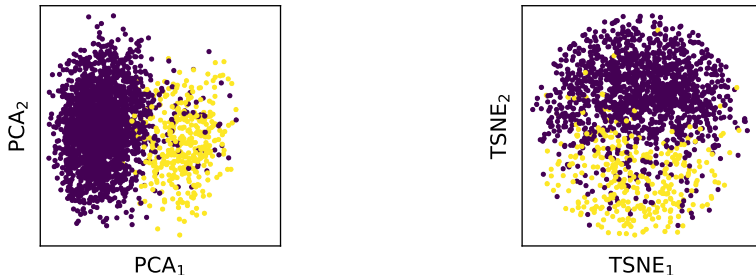

Figure 5: **Separability of meta-stable States in latent space.** Transforming molecule conformations following the states C_5 and α_R into the latent space, and plotting them in 2D with PCA and TSNE. The colors indicate the different conformations.

C   The Test System Alanine Dipeptide

To run our experiments, we relied on the molecule alanine dipeptide. Although it has 22 atoms, it is mostly described by its two main dihedral angles ϕ, ψ. Figure 6 illustrates the histogram of these angles.

D   Determining the Timestep for TPS

Finding out the transition time between two states is necessary to be able to determine a suitable timestep Δt and the number of frames. While this task can be challenging for large systems, this is not a task we set out to solve. To determine meaningful values, we have estimated the density of the transition times as they occur in a long-running MD simulation, as can be seen in Figure 7. With
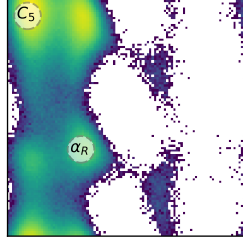
Figure 6: Distribution of alanine dipeptide's 3D configurations visualized via a histogram of its main dihedral angles ϕ, ψ. Two metastable states are highlighted, between which we aim to sample the ensemble of all possible transition paths.

this, we have decided to sample transition paths with a duration of $1.6ps$. Similar studies can be performed to determine the transition times with high probability for transitions between α_R and C_7, where we decided to use a time of $320fs$.
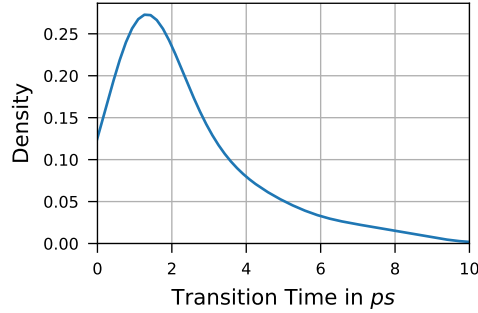

Figure 7: **Duration of ALDP transitions.** This is the approximated density that shows the duration of the transition between the states C_5 and α_R and their respective densities.

E Latent Hamiltonian Dynamics Kernel

In this section, we introduce another latent proposal kernel that independently performs Hamiltonian MCMC [Duane et al., 1987, Neal, 2011] in latent space. The main idea was introduced by Hoffman et al. [2019], and we extend it to transition paths. The major advantage of this approach is that the gradient of a well-conditioned latent space, such as a Gaussian, can be evaluated efficiently.

For this, we perform L leapfrog integration steps with a step size of ϵ. The algorithm initializes the variables

$$
\begin{aligned}
\boldsymbol{m}_i^{(0)} &= \boldsymbol{m}_i + (\epsilon/2)\nabla p_Z(\boldsymbol{z}_i), \\
\boldsymbol{z}_i^{(0)} &= \boldsymbol{z}_i,
\end{aligned}
\tag{11}
$$

and samples a random momentum $\boldsymbol{m}_i \sim \mathcal{N}(0, \mathbb{1}^D)$. ∇p_Z is the gradient in the latent space, which in our case is a standard normal distribution. Then we perform L leapfrog steps to update

$$
\begin{aligned}
\boldsymbol{z}_i^{(t+1)} &= \boldsymbol{z}_i^{(t)} + \epsilon \boldsymbol{m}_i^{(t)}, \\
\boldsymbol{m}_i^{(t+1)} &= \boldsymbol{m}_i^{(t)} + \epsilon \nabla p_Z(\boldsymbol{z}_i^{(t+1)}),
\end{aligned}
\tag{12}
$$

for $t \in [0, 1, \ldots, L-1]$. We conclude the steps by a final update

$$
\begin{aligned}
\boldsymbol{z}_i^* &= \boldsymbol{z}_i^{(L)}, \\
\boldsymbol{m}_i^* &= \boldsymbol{m}_i^{(L)} - (\epsilon/2)\nabla p_Z(\boldsymbol{z}_i^{(L)}).
\end{aligned}
\tag{13}
$$

11

Contrary to the other kernels presented in this paper, this proposal is not symmetric anymore. The proposal ratio is a straightforward extension of Hoffman et al. [2019] and can be written as

$$\frac{q_Z(\boldsymbol{z} \mid \tilde{\boldsymbol{z}})}{q_Z(\tilde{\boldsymbol{z}} \mid \boldsymbol{z})} = \prod_{i=1}^{l} \frac{p_Z(\boldsymbol{m}_i^*)}{p_Z(\boldsymbol{m}_i)} = \prod_{i=1}^{l} \frac{\mathcal{N}(\boldsymbol{m}_i^* \mid 0, \mathbb{1})}{\mathcal{N}(\boldsymbol{m}_i \mid 0, \mathbb{1})}. \tag{14}$$
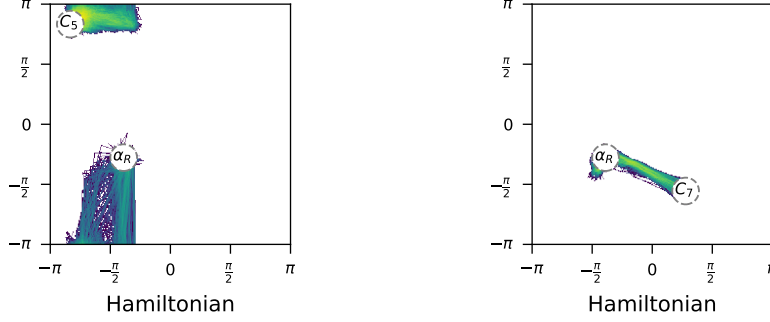
Figure 8: **Latent Hamiltonian Proposal Kernel.** The resulting path histograms when simulating the evolution of the samples in latent space according to the Hamiltonian dynamics.

F   Impact of Variance on Latent Noise Proposal Kernel

The variance of the noise added in latent space is a hyperparameter that will impact the similarity of generated paths. The smaller the variance, the more similar the produced paths will be. In Figure 9, we investigate different noise scales. We can see that a larger variance produces a more diverse ensemble of paths, but the runtime of our approach will increase with it as most proposals will be rejected. This is a trade-off similar to what can be observed in shooting-based TPS, where moves with a vastly different velocity will likely not produce paths with a high probability.
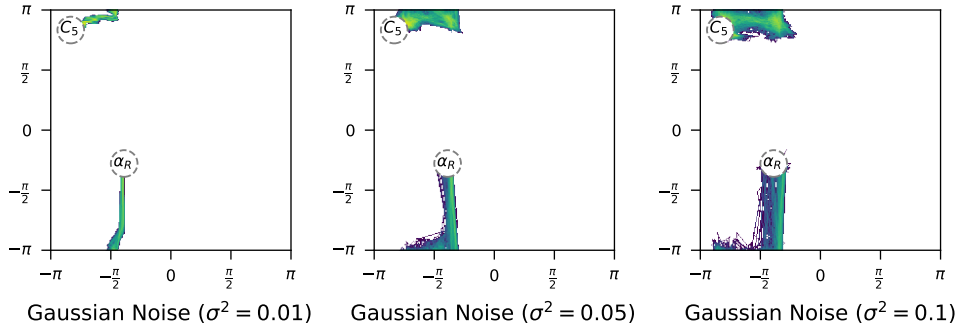
Figure 9: **Linear latent proposal kernel with different variances.** We compare three different path ensembles sampled by applying noise to the frames in latent space. The noise was sampled from a zero-mean normal distribution with a different σ^2.